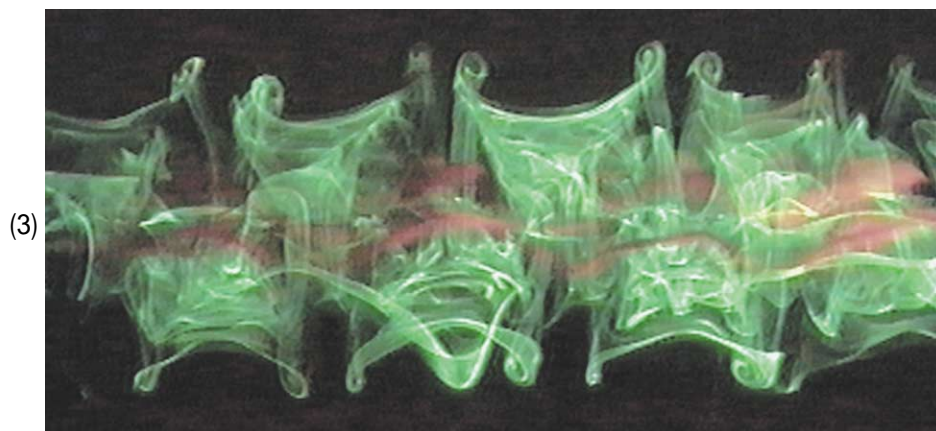
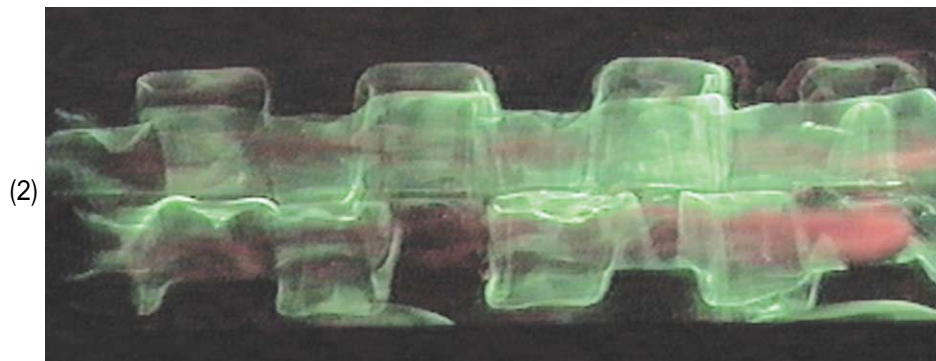
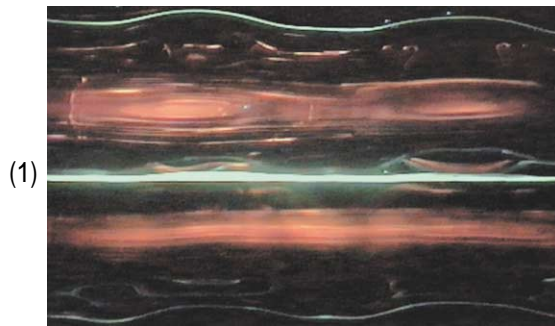


1. Secondary Structures in a Corotating Vortex Pair

Meunier, P.¹⁾ and Leweke, T.¹⁾

1) Institut de Recherche sur les Phénomènes Hors Equilibre (IRPHE), 49 rue F. Joliot-Curie, B.P. 146
F-13384 Marseille Cedex 13, France



This sequence shows the evolution of two perturbed corotating vortices, generated in water using impulsively moved flat plates. The Reynolds number based on the circulation of one vortex is approximately 3000. The vortex cores are visualized using red dye (Rhodamin B), painted on the plate edges. In addition, a nylon thread coated with green fluorescent dye is placed in the middle between the two vortex centers (1). Illumination is achieved in a sheet (1) or in volume ((2) and (3)), using light from an Argon laser, and the flow is observed from the side, i.e. perpendicular to the vortex axes (the field of view is approx. 25 cm wide in (2) and (3)). The corotating vortices, which in their basic state rotate around each other, are perturbed by adding a sinusoidal deformation to the edge of the vortex-generating plates. This creates a periodic perturbation of vorticity between the vortices, near the dyed thread, where the basic flow exhibits a hyperbolic stagnation point. The corresponding strain stretches the vorticity perturbation into secondary vortex pairs, which are perpendicular to the primary vortices. At an early stage, this process leads to the peculiar square dye patterns in (2). In (3), taken about half a rotation period of the primary pair later, the secondary vortex pairs are clearly visible, as they now wrap around the outside of the corotating pair. The presence of the secondary structures amplifies the wavy deformation of the primary vortex cores, which are still visible in red. At a later stage, the two primary vortices merge into a single one, and the interaction with the perpendicular secondary vortices leads to a rapid breakdown of the flow into turbulent small-scale structures.

2. Imaging the Terrestrial Plasmasphere by the XUV Scanner from Space

Nakamura, M.¹⁾, Shiomi, K.¹⁾, Yoshikawa, I.²⁾, Yamazaki, A.³⁾, Miyake, W.³⁾, Takizawa, Y.⁴⁾ and Yamashita, K.⁵⁾

1) Earth and Planetary Sciences, Graduate School of Science, The University of Tokyo, 7-3-1, Hongo, Bunkyo, Tokyo 113-0033, Japan

2) Institute of Space and Astronautical Science, 3-1-1 Yoshinodai, Sagami, Kanagawa 229-8510, Japan

3) Communications Research Laboratory, 4-2-1, Nukui-Kitamachi, Koganei, Tokyo 184-8795, Japan

4) Division of Image Information, Advanced Computing Center, Institute of Physical and Chemical Research, 2-1, Hirosawa, Wako, Saitama 351-0198, Japan

5) Department of Physics, Nagoya University, Furouchou, Chikusa, Nagoya 464-8602, Japan

An extreme ultraviolet (XUV) scanner on board the Mars orbiter, Planet-B, observed the terrestrial plasmasphere while it was in a parking orbit around the earth. This was the first image from space (Nakamura, et al., 2000; Yoshikawa, et al., 2000). The helium ions populated in the terrestrial plasmasphere resonantly scatter the solar EUV rays at 30.4 nm. Therefore, the global imaging resulting from detection of 30.4 nm HeII emission represents the structure of the terrestrial plasmasphere. The visualization of the plasmasphere has been a long-cherished goal in magnetospheric physics.

The key technology of the scanner is the multi-coated Mo/Si mirror, which reflects preferentially EUV rays at 30.4 nm. The reflectivity shown in Fig. 1 gives the peak at 30.4 nm, where the reflectivity is enhanced to 18%.

Fig. 2 shows the EUV image of the dusk-side terrestrial plasmasphere on September 9-10, 1998. With the spacecraft's motion along its orbit, the telescope scanned the whole plasmasphere. The field of view of the telescope is 3.2 degrees, which corresponds to 1,800 km spatial resolution when the target is observed 5Re (earth radius) away. The lines in the images are magnetic field lines of L=4 and 6 (L is the L shell parameter which gives the distance from the earth's center to the dipole field line at equator divided by earth radius). The signal was as strong as 6.3Rayleigh (where 1Rayleigh= 10⁶photons/cm²/sec) at L=4. Surprisingly, many helium ions are distributed beyond the L=6 field line. This finding appeals us to challenge further global EUV imaging.

References:

1. Nakamura, M., Yoshikawa, I., Yamazaki, A., Shiomi, K., Takizawa, Y., Hirahara, M., Yamashita, K., Saito, Y. and Miyake, W., Terrestrial Plasmaspheric Imaging by an Extreme Ultraviolet Scanner on Planet-B, *Geophys. Res. Lett.*, 27, (2000), 141-144.
2. Yoshikawa, I., Yamazaki, A., Shiomi, K., Yamashita, K., Takizawa, Y. and Nakamura, M., Evolution of the outer plasmasphere during low geomagnetic activity observed by the EUV scanner onboard Planet-B, *J. Geophys. Res.*, (2000), 105, 27,777-27,789.

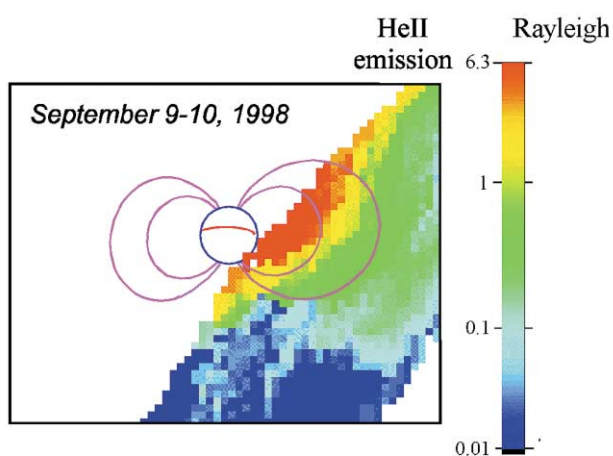


Fig. 1

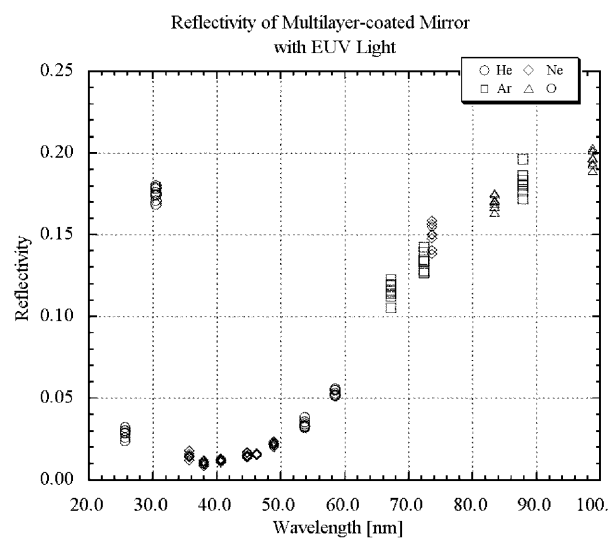


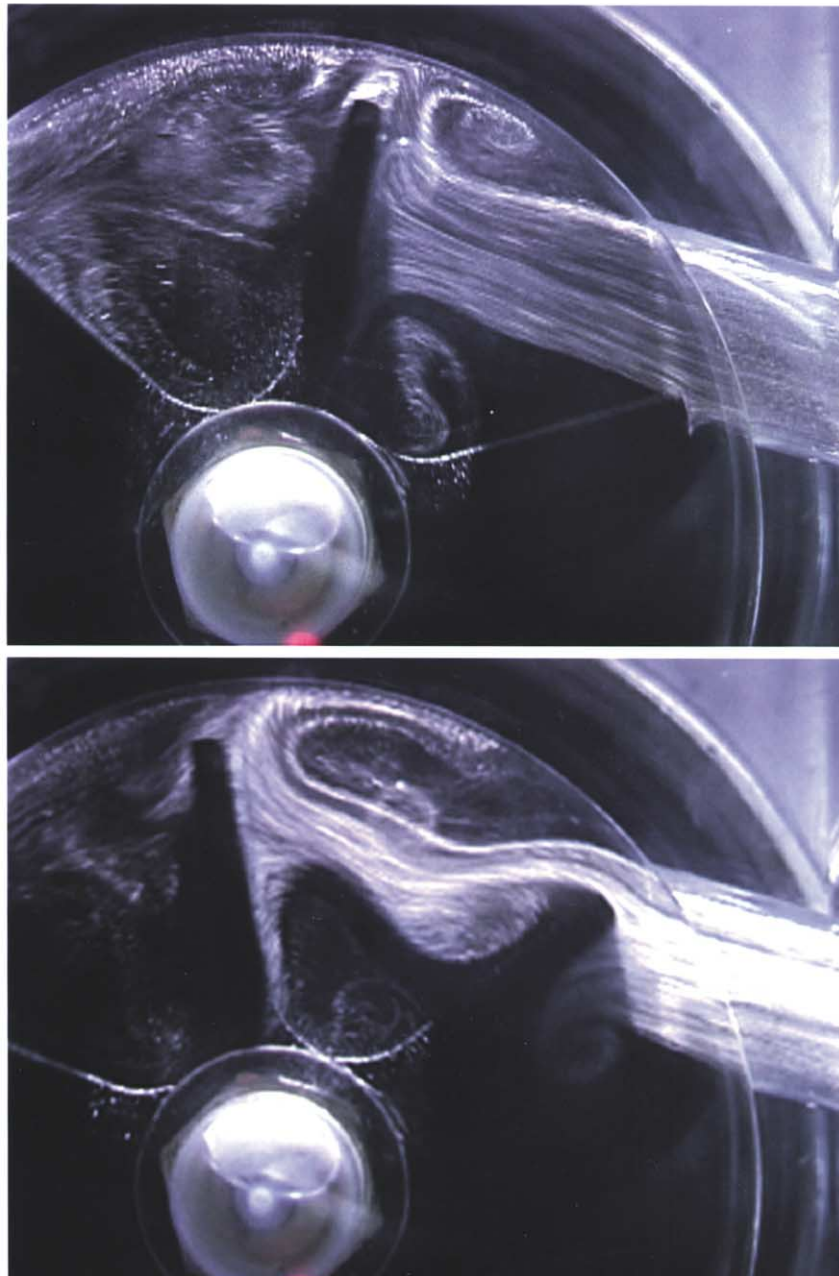
Fig. 2

3. Flow Field in a Rotating Vane Flow Meter

Oshima, Y.¹⁾ and Takamiya, T.²⁾

1) RDC Ricoh Co., Ltd. 16-1, Shineicho, Tsuzuki-ku, Yokohama 224-0035, Japan

2) Ricoh Elemex Corporation, 1-9-17, Oomori Nishi, Oota-ku, Tokyo 143-0015, Japan

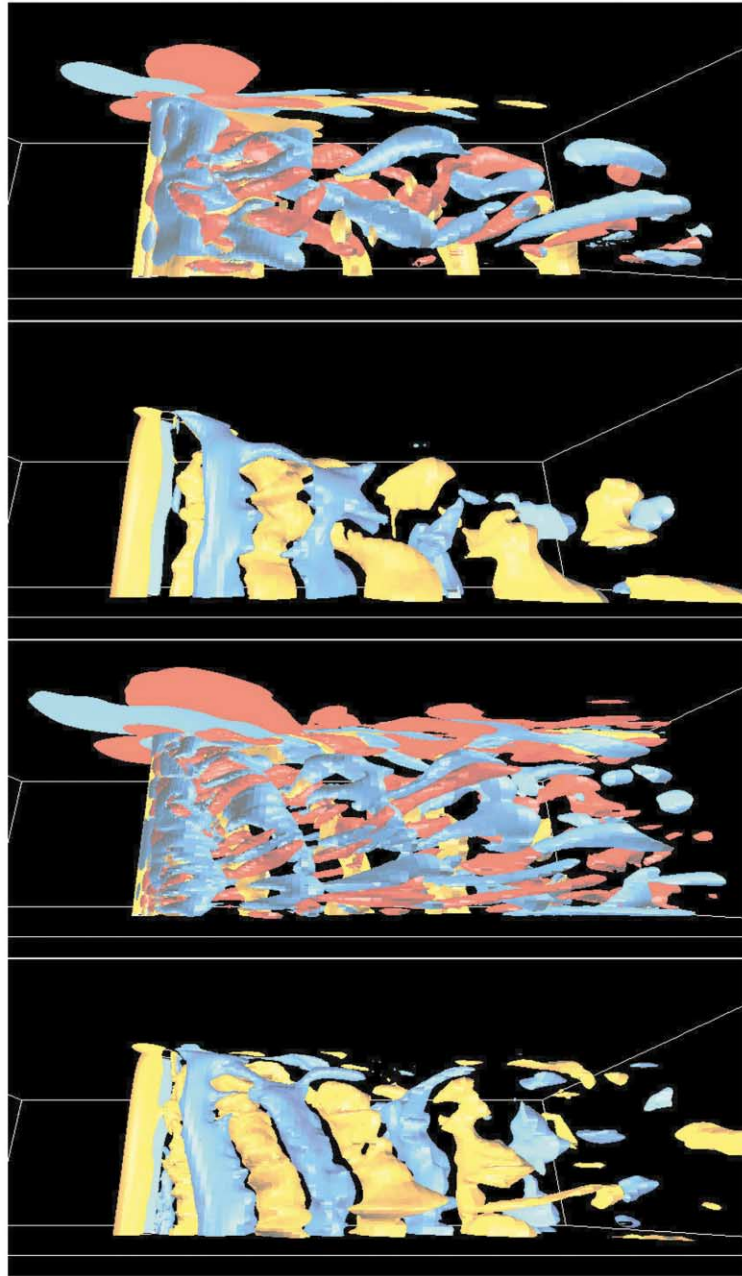


The flow field in a rotating vane flow meter is visualized by hydrogen bubble method. The meter is the size of 5.8 cm in diameter and 2.5 cm in height. Rotor with 6 vanes rotates due to inlet flow and the number of rotation is proportional to the flow quantity. The flow from the inlet makes a pair of vortices in a space between the vanes, and the vortices flow out from the outlet. The photographs are taken with 1/4 cycle difference at the cross section of the center of vane height using sheet light. Flow rate is 25L/H, and the Reynolds number based on the inlet diameter is about 800.

4. 3D Flows Past Circular Cylinder of Low Aspect Ratio

Mittal, S.¹⁾, Bankoti, H.¹⁾ and Dhananjay, G.¹⁾

1) Department of Aerospace Engineering, Indian Institute of Technology, Kanpur, UP 208 016, India



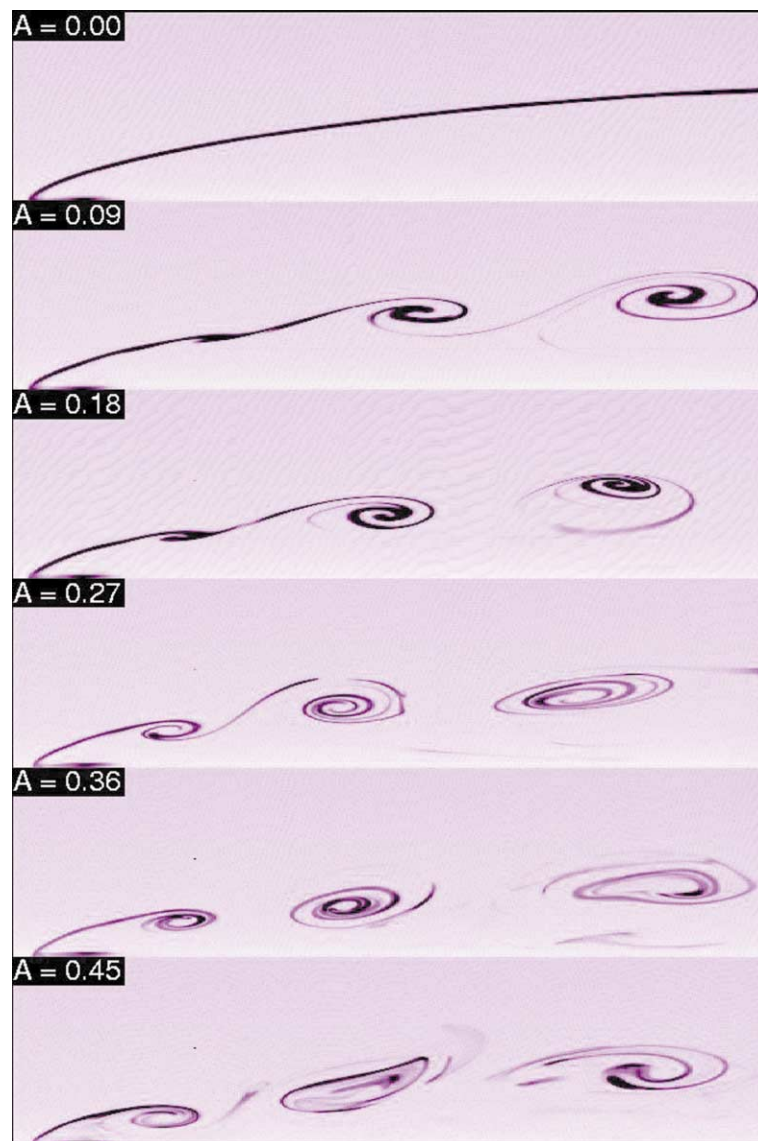
Flows past finite cylinders of low aspect ratio (length to diameter ratio=16) are studied using finite element simulations. The end-conditions are specified to model the effect of a "no-slip" wall. Only one half of the spanwise length is considered. At $Re=300$ Mode A and Mode B patterns of vortex shedding in addition to vortex dislocations are observed at different time instants. The wake transition regime, which is known to occur in the Re range 190-250 for large aspect-ratio cylinders, is either extended and/or delayed for a cylinder of small aspect ratio with "no-slip" walls. At $Re=1000$ Mode B is observed along with vortex dislocations. The "no-slip" walls result in oblique mode of vortex shedding.

The top two frames are for $Re=300$ while the lower ones for $Re=1000$ flow. The first and third frames show the isosurfaces of the streamwise (ω_x) and spanwise (ω_z) vorticity field [red: $\omega_x=0.2$, blue: $\omega_x=-0.2$, yellow: $\omega_z=0.3$]. The second and fourth frames show the isosurfaces of the crossflow component of velocity field [blue: $v=-0.2$, yellow: $v=0.2$].

5. The Structure of a Separated Shear Layer from a Blunt Leading Edge under Forcing

Panchapakesan, N.R.¹⁾ and Soria, J.¹⁾

1) Laboratory for Turbulence Research in Aerospace and Combustion, Department of Mechanical Engineering, Monash University, Melbourne, VIC 3800, Australia



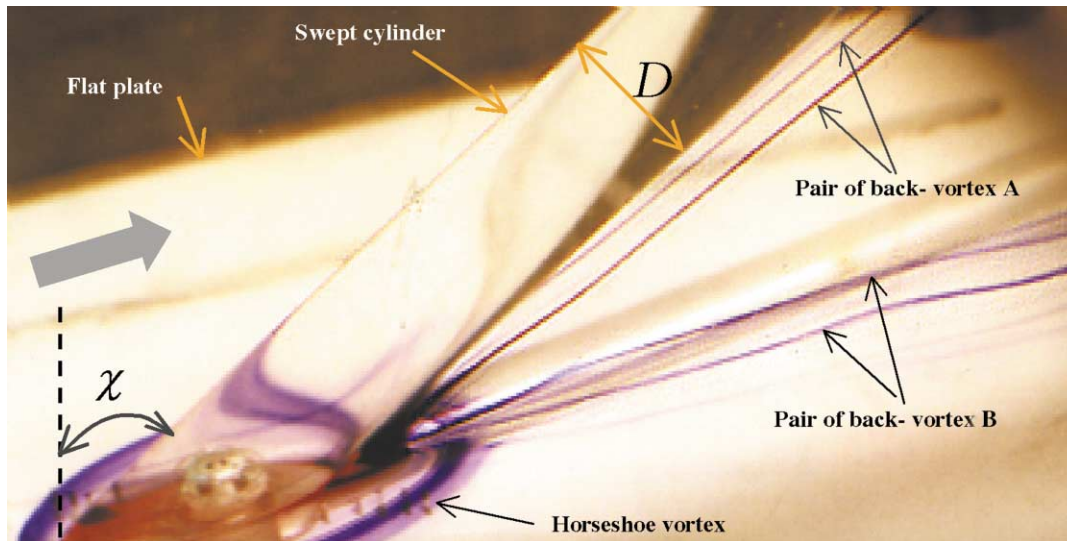
The development of a separated shear layer from a blunt leading edge normal to the flow was visualized with a fluorescing dye. A flat plate of width 25 mm and size 500 mm by 500 mm was placed in a water tunnel. A slit of 0.5 mm width and 100 mm length at the center of the leading edge was used to force the shear layer. The slit was 4 mm to one side of the center line. A scotch yoke mechanism connected to an hydraulic cylinder was used for imposing harmonic disturbances on the shear layer through the slit. The fluorescing dye was injected through an orifice of 0.5 mm diameter and displaced 5 mm from the slit. A laser sheet with a pulse duration of 6 ns and 2 mm thickness located transverse to the plate was used for illumination. The flow velocity was 35 mm/s and the Reynolds number was 1000.

The sequence of six images in the photograph show the development of the shear layer for different amplitudes of excitation normalized by the flow velocity A . The flow is from left to right. The separation corner is at the lower left corner of the image which depicts an area of 20 mm by 58 mm. The first image shows the shear layer without forcing and the remaining images show the effect of forcing at 1 Hz at various amplitudes. Strong non-linear development of vortical structures that penetrate the separated region can be clearly seen in the forced cases. The effect of these structures on the mass, momentum and heat transfers can be exploited to control the flow.

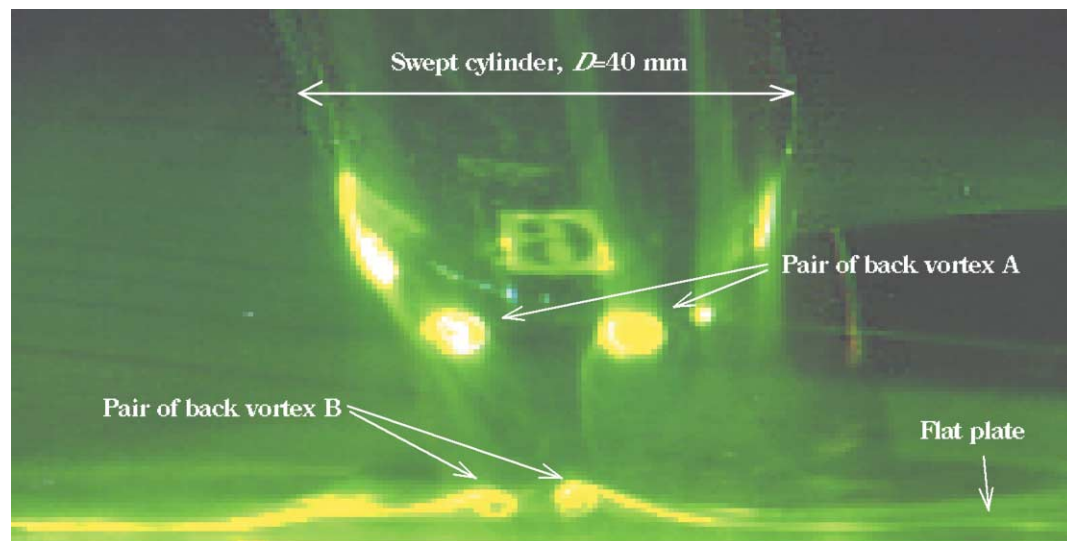
6. The Back-vortex System in Swept Cylinder/Flat Plate Interactions

Hua, Z.¹⁾

1) Fluid Mechanics Institute (FMI), Beijing University of Aeronautic and Astronautics (BUAA), Beijing 100083, China



The side view of back-vortex system in swept cylinder/flat plate interactions, diameter $D=40$ mm, swept angle $\chi=60^\circ$



The back view of back-vortex system in swept cylinder/flat plate interactions, diameter $D=40$ mm, swept angle $\chi=60^\circ$

The cylinder/flat plate junction presents the simplest juncture flow interactions. It is well known that the adverse pressure gradient supplied by the model would cause the horseshoe vortex system in front of and round the model.

For the swept-cylinder/flat-plate interactions, there exists another kind of 3-D space vortex system---back-vortex. There are two sets (pair) of back-vortices, one close to the swept cylinder (labeled back-vortex A), and another close to the flat plate (labeled back-vortex B). The axes of back-vortex A and B start from the back corner of the juncture and extend to downstream. The back-vortices are essentially stable and the periodical oscillating or shedding off phenomena is not observed. The mechanism of forming back-vortex is virtually similar to that of horseshoe vortex except the source of the vortex vorticity. The back-vortex A would break-down under smaller swept angle. The back-vortex B might interact with the two legs of horseshoe vortex and wrap into a new vortex.